13th Australasian Fluid Mechanics Conference
Monash University, Melbourne, Australia
13-18 December 1998

MULTIGRID APPROACH TO CROSS-CORRELATION DIGITAL PIV AND HPIV ANALYSIS

Julio Soria

Department of Mechanical Engineering
Monash University, Clayton, Melbourne, Victoria, AUSTRALIA

ABSTRACT

A new method of cross-correlation digital PIV (CCDPIV) analysis of two single-exposed images based on a multigrid approach is presented in this paper. Multigrid CCDPIV (MCCDPIV) analysis is an evolution of the adaptive CCDPIV analysis method (Soria(1996b) and can be used to interrogate two single-exposed digital, photographic or hologram recordings of seed particles in a fluid flow containing a large range of velocity and length scales without *a priori* knowledge of the flow and with minimal user intervention. A comparative investigation of the accuracy between MCCDPIV and standard CCDPIV processing has been carried out using computer generated digital images with known velocity (displacement) fields.

INTRODUCTION

This paper describes a new approach to cross-correlation digital particle image velocimetry (CCDPIV) analysis which extends the dynamic range of the displacement measurements and simultaneously improves the spatial resolution of the measured velocity field. The novel methodology is based on a *multigrid* approach to CCDPIV analysis. The multigrid CCDPIV (MCCDPIV) idea is an evolution of the adaptive CCDPIV analysis method proposed by Soria(1996b), which in principle permits better parallelisation than the original adaptive CCDPIV analysis method.

The requirement for a adaptive CCDPIV originally arose in the context of a requirement for PIV velocity measurements in the near wake of a circular cylinder. The flow field in the near wake has thin shear layers emanating from the separation point on the cylinder that effectively divide the flow field into a high speed flow domain (*i.e.* the free-stream domain) and a low speed flow domain (the immediate region downstream of the cylinder surface). The flow in the low speed domain is recirculating and highly unsteady with the shear layers subject to instabilities and "*flapping*".

The near wake of a circular cylinder is only an example of a unsteady, transitional or fully turbulent flows, which can be characterised by:

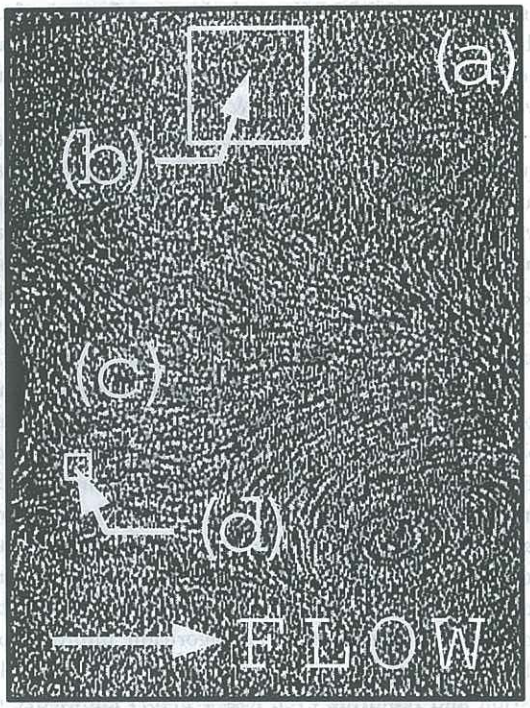

Figure 1: Flow visualisation of the near wake downstream of a circular cylinder at Reynolds number of 500, showing the relative seed particle displacements between the high speed regions - (a) and the low speed regions - (c). (b) is an interrogation window with SWS = 128 px while (d) corresponds to SWS = 32 px.

- a wide range of velocity scales
- thin shear layers which are often unstable (or equivalently a large range of length scales)
- and (possibly) recirculating flow.

It is obvious that high spatial resolution is essential in the acquisition of the seed particle images in order to resolve the large velocity gradients in the shear layers and the wide range of length scales. It is also quite apparent that cross-correlation digital PIV (CCDPIV) analysis of single-exposed images is essential to measure the in-plane flow field without *a priori*

assumption of the flow field and minimal intervention by the experimentalist (Soria *et al.* (1998)). Both these requirements are desirable to minimise possible bias in the measurements.

The most common image acquisition technique of single-exposed images uses digital CCD cameras, which imposes strict limits on the available spatial resolution limit due to their current technology. One method of circumventing this limitation is to use high spatial magnification at the expense of a reduced recorded flow domain. This approach results in very large displacements of the seed particles in the high speed region, see Fig. 1. The problem in analysing the two single-exposed images of this flow using standard CCDPIV analysis arises from the fact that in practice, the maximum displacement that can be measured is limited to 0.25 - 0.3 of the sampling window size (SWS) (Keane & Adrian(1990)).

Figure 1 illustrates the problem, showing the required sampling window with SWS = 128 px for measurements in the high speed region and the sampling window with SWS = 32 px which is sufficient for measurements in the low speed region. Clearly, this latter sampling window provides higher spatial resolution measurements, but will not yield any measurements in the high speed region.

The adaptive CCDPIV algorithms proposed and developed by Soria(1996b), Soria(1996a) uses sampling windows that adapt in size to the local flow conditions, in addition to implementing an adaptive discrete sampling window offset of the sampling window in the second exposure. These processes are fully automatic without operator intervention and with minimal *a priori* knowledge of the velocity field to be measured. The MCCDPIV algorithm improves on that algorithms by allowing more efficient parallelisation and requiring even less *a priori* knowledge of the flow field to be measured.

MULTIGRID CROSS-CORRELATION DIGITAL PIV

The basic MCCDPIV analysis algorithm is based on setting up a hierarchy of grid levels, each with a specific SWS as illustrated in Fig. 2. The $0th$ grid level has the largest SWS, SWS_0 px, the $1st$ grid level has a smaller SWS, SWS_1 px. Grid levels are established down to the nth grid level which has a SWS equal to SWS_n px.

The MCCDPIV algorithm then proceeds as follows:

1. CCDPIV analysis at the $0th$ grid level using SWS = SWS_0 px:
   (a) analyse the two single-exposed images on the $0th$ grid level using a SWS = SWS_0 - this step determines all the large magnitude displacements and provides smoothed estimates of smaller magnitude displacements
   (b) the quality and consistency of the displacement estimates at the $0th$ grid level is checked.
2. CCDPIV analysis at the $1th$ grid level using SWS = SWS_1 px:
   (a) estimate the local displacements at the centre of the sampling windows of the $1st$ grid level using the $0th$ grid level CCDPIV measurements
   (b) if an estimated displacement exists and is larger than 0.5 px, then use the estimated displacement to discretely offset the sampling window in the second exposed image as shown in Fig. 3, otherwise no offset is used
   (c) CCDPIV analysis with SWS = SWS_1 px is then performed between the sampling window fixed to the $1st$ grid level centre of the sampling window in the first exposed image and the offset sampling window in the second exposed image
   (d) the quality and consistency of the displacement estimates at the $1th$ grid level is checked once the CCDPIV analysis of all sampling windows at this grid level is completed
3. CCDPIV analysis down to the nth grid level with SWS = SWS_n proceeds using the same steps for each grid level as described for $1st$ grid level, except that the discrete offset displacement is estimated from the previous grid level.

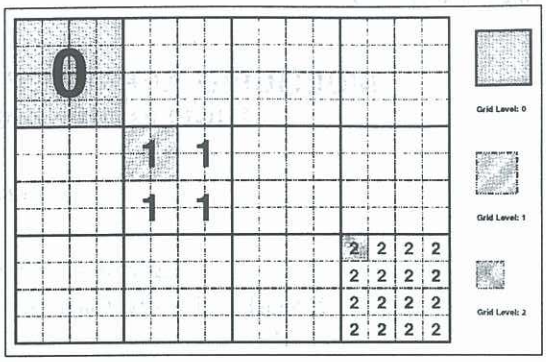

Figure 2: Schematic showing the hierarchy of grid size levels for Multigrid CCDPIV.

An additional option to the above algorithm is to apply a smaller sampling window in the first exposure during the CCDPIV analysis at each grid level. This feature is schematically illustrated in Fig. 4 for the $0th$ grid level. A reasonable size for this smaller sampling window is the size of the smallest sampling

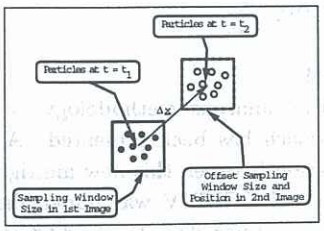

Figure 3: Schematic illustrating offset CCDPIV sampling windows.

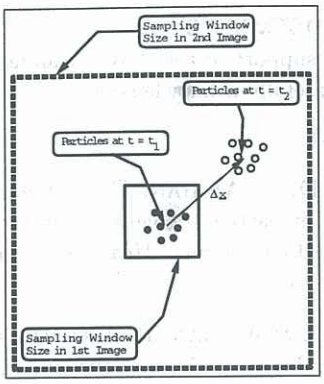

Figure 4: Schematic showing the differential SWS used for CCDPIV analysis.

window, SWS_n px to be used in the MCCDPIV analysis.

The MCCDPIV algorithm is ideally suited for parallel processing because at each grid level the CCDPIV analysis of each individual sampling region can be carried out independent of the other sampling regions. In principle the CCDPIV analysis of each sampling region can be carried out by a separate processor. Thus, each processor performs exactly the same work load and the CCDPIV computation is synchronised on all processor.

The CCDPIV analysis output of all individual sampling regions from all processor, which in principle is available at the same instant, is only required for the quality and consistency checking stage. At grid levels higher than the $0th$ level the entire stage 2 except for 2(d), the quality and consistency checking stage, can also be performed with the same optimum parallelisation.

PERFORMANCE OF MCCDPIV

The performance and accuracy of the MCCDPIV analysis has been comparatively investigated to standard CCDPIV using computer generated digital images. Square digital images with a size of 1200^2 px^2 containing 56256 randomly positioned particle images have been generated. The intensity distribution of the particle images is assumed to be Gaussian (Keane & Adrian(1992)) with an effective diameter of 1.25 px. Uniform displacement fields of (3.2 px, -3.2 px) and (32.3 px, 32.3 px) have been employed for the comparative investigation.

Offset CCDPIV Accuracy Results.

In the discrete sampling window offset CCDPIV analysis, where the sampling window in the second image is displaced by a discrete estimate of the displacement such that the residual displacement is less than 0.5 px in either orthogonal coordinate direction, results in a reduced random displacement measurement error. This was noted in the early development of the adaptive CCDPIV method (Soria(1994)) and recently investigated in detail by Westerweel *et al.* (1997).

Table 1 summarises the standard deviation of the random error of the displacement measurements using CCDPIV analysis and CCDPIV analysis with discrete sampling window offset. The results in this table demonstrate that the discrete offset of the sampling window in CCDPIV analysis reduces the random error by approximately a factor of 2. The reduction in the random error for larger sampling window sizes presented in Table 1 is due to the increased number of sampled particles available for CCDPIV analysis in the larger sampling windows. The corresponding probability density functions (PDF) of the random error for the results in Table 1 are presented in Fig. 5. These PDFs show that the random error has an approximately Gaussian distribution.

Sampling Window Size	Standard CCDPIV			Standard CCDPIV followed by Offset CCDPIV		
	Fraction of Good Vectors	$\sigma_{\Delta x}$	$\sigma_{\Delta y}$	Fraction of Good Vectors	$\sigma_{\Delta x}$	$\sigma_{\Delta y}$
px		px	px		px	px
32	0.998	0.064	0.063	0.992	0.028	0.029
64	0.988	0.028	0.024	0.996	0.016	0.016

Table 1: Comparison of uncertainty for standard CCDPIV and standard CCDPIV followed by offset CCDPIV.

Multigrid CCDPIV Accuracy Results.

The performance of the MCCDPIV analysis compared to standard CCDPIV analysis was specifically investigated by using displacements which were larger than 0.5 of the smallest SWS in the MCCDPIV analysis. The comparative results are presented in Table 2. A two grid level MCCDPIV analysis was used. The $0th$ grid level had a $SWS_0 = 128$ px, and $1st$ grid level either had a $SWS_1 = 32$ px for small displacement or 64 px for large displacement. Note that it is not necessary to have a full hierarchy of grid levels with grid sizes which differ by a factor of 2.

It is worth noting that for **small displacements**, MCCDPIV with a smaller SWS than the standard CCDPIV has a smaller random error and provides marginally more *good* displacement vector measurements. The advantage of the MCCDPIV algorithm is more obvious in the case of **large displacements**, where the standard CCDPIV analysis requires sampling windows which are 3 – 4 times

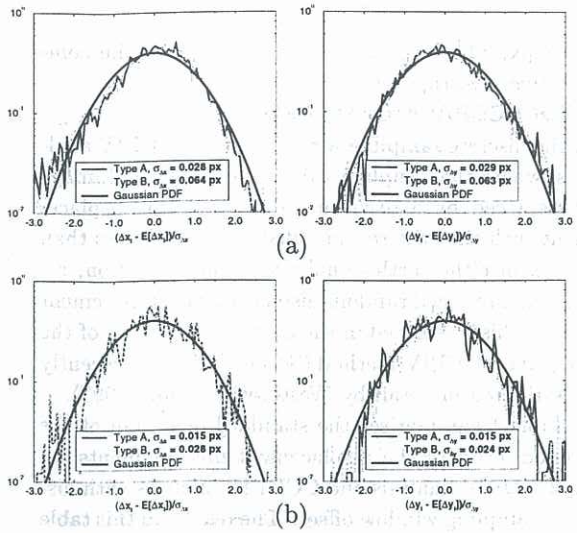

Figure 5: PDF of random error of horizontal and vertical displacement measurements for standard CCDPIV analysis (Type B) and standard CCDPIV followed by offset CCDPIV analysis (Type A). The results in (a) correspond to analysis with SWS = 32 px and (b) correspond to analysis with SWS = 64 px.

Uniform Displacement Δx, Δy px	Standard CCDPIV SWS px	σ_u px	σ_v px	Multigrid CCDPIV Smallest SWS px	σ_u px	σ_v px
SMALL DISPLACEMENTS						
3.2, 3.2	32 (0.998)	0.064	0.064	32 (0.996)	0.017	0.017
3.2, 3.2	64 (0.988)	0.028	0.028	–	–	–
LARGE DISPLACEMENTS						
32.3, 32.3	96 (0.999)	0.054	0.055	64 (0.997)	0.021	0.021
32.3, 32.3	128 (0.998)	0.033	0.032	–	–	–

Table 2: Uncertainties determined from uniform displacement tests. The number in brackets is the fraction of *good* measurements to total number of possible measurements.

larger than this displacement to avoid the problem of too many particles having left the sampling window area in the second image recording (Keane & Adrian(1990)). Due to the high particle density in the digital images it is still possible to measure the **large displacement** with SWS = 96 px. However as the results in Table 2 show, standard CCDPIV analysis with SWS = 128 px reduces the random error. Standard CCDPIV analysis with SWS = 64 px results in 100% erroneous measurements. However, MCCDPIV with the smallest SWS = 64 px results in a *good* displacement measurement rate of 0.997 with a random error equal to 0.6 of that of the standard CCDPIV analysis with SWS = 128 px.

Thus, MCCDPIV provides measurements with lower random error, a higher dynamic measurement range and because smaller sampling window can be employed, MCCDPIV analysis also provides measurements with higher spatial resolution compared to standard CCDPIV.

CONCLUSION

A new CCDPIV analysis methodology based on a multigrid approach has been presented. A comparative investigation between this new multigrid CCDPIV and standard CCDPIV was undertaken. MCCDPIV analysis compared to standard CCDPIV provides displacement (*i.e.* velocity) measurements with lower random error, larger dynamic measurement range and higher spatial resolution.

ACKNOWLEDGEMENTS

The financial support of the ARC to undertake this research is gratefully acknowledged.

REFERENCES

KEANE, R. D. & ADRIAN, R. J. (1990). Optimisation of particle image velocimetry. Part I: Double pulsed systems. *Meas. Sci. Technol.* **1**, 1202 – 1215.

KEANE, R. D. & ADRIAN, R. J. (1992). Theory of cross-correlation analysis of PIV images. *Appl. Sci. Res.* **49**, 191 – 215.

SORIA, J., , KOSTAS, J., FOURAS, A., & CATER, J. (1998). A high-spatial resolution and large dynamic range cross-correlation PIV technique for turbulent flow measurements. In *Optical methods and Data Processing in Heat and Fluid Flow* pp. 375–384 London, U.K. IMechE Conference Transactions.

SORIA, J. (1994). Digital cross-correlation particle image velocimetry measurements in the near wake of a circular cylinder. In *International Colloquium on Jets, Wakes and Shear Layers* Melbourne, Australia.

SORIA, J. (1996a). An adaptive cross-correlation digital PIV technique for unsteady flow investigations. In *Proc. 1st Australian Conference on Laser Diagnostics in Fluid Mechanics and Combustion* (eds. A.R. Masri and D.R. Honnery) Sydney, NSW, Australia. University of Sydney University of Sydney.

SORIA, J. (1996b). An investigation of the near wake of a circular cylinder using a video-based digital cross-correlation particle image velocimetry technique. *Experimental Thermal and Fluid Science* **12**, 221 – 233.

WESTERWEEL, J., DABIRI, D., & GHARIB, M. (1997). The effect of a discrete window offset on the accuracy of cross-correlation analysis of digital PIV recordings. *Expt. Fluids* **23**, 20 – 28.